NANO LETTERS

2004
Vol. 4, No. 6
1063−1066

Hot Carrier Electroluminescence from a Single Carbon Nanotube

Marcus Freitag,[†,‡] Vasili Perebeinos,[†] Jia Chen,[†] Aaron Stein,[§] James C. Tsang,[†] James A. Misewich,[§] Richard Martel,[†,||] and Phaedon Avouris*[,†]

IBM Research Division, T. J. Watson Research Center, Yorktown Heights, New York 10598-0218, Carbon Nanotechnologies, Inc., 16200 Park Row, Houston, Texas 77084, and Brookhaven National Laboratories, Upton, New York 11973

Received March 11, 2004; Revised Manuscript Received April 2, 2004

ABSTRACT

We measure the spectrum and efficiency of the infrared light emission from ambipolar carbon nanotube field-effect transistors. The width of the emission peak is strongly device-structure dependent. Long devices (∼50 μm) show narrow spectral peaks that we attribute to relaxed carrier recombination, while short devices (∼500 nm) show broad peaks due to hot carrier recombination. The hot carrier distribution is limited to energies below the energies of the optical/zone boundary phonons near 180 meV. The efficiency of the radiative recombination is between 10^{-6} and 10^{-7} photons/electron–hole pair, and the possible quenching mechanisms are discussed.

Carbon nanotubes (CNT) are one-dimensional systems that make excellent candidates for future nanoelectronic applications.[1,2] CNTs are also direct gap materials and as such may find applications in nanophotonics.[3,4] Recently we demonstrated electrically induced optical emission from a single carbon nanotube acting as the channel of an ambipolar field-effect transistor (FET).[3] Schottky barriers at the metal contacts allow electron injection at one terminal and hole injection at the other.[5−7] The carriers can then recombine radiatively or nonradiatively in the carbon nanotube. Here we present the spectral distribution of the emitted infrared light. We determine the carrier energy distribution in the carbon nanotube and the efficiency of the radiative recombination process.

Laser ablation grown ambipolar CNT-FETs with channel lengths on the order of 500 nm were fabricated with titanium-carbide contacts as described in ref 5. The devices are covered with a low-temperature silicon-oxide (LTO) and annealed at 800 °C to drive out any oxygen from the contact region. This makes the band-lineup roughly mid-gap and the devices ambipolar.[5,8] CVD-grown CNT-FETs with channel lengths varying between 400 nm and 80 μm were contacted by palladium without post-processing. The band lineup in these devices is closer to the valence band,[9] but electron injection is also possible and the devices show ambipolar behavior. Infrared emission from the CNT-FET was detected by a liquid nitrogen cooled HgCdTe detector array, mounted on top of the camera port of an optical microscope. Spectra were obtained using optical band-pass filters with spectral widths between 40 and 90 nm.

Figure 1a shows a schematic of the device. Electrons and holes are injected from opposite contacts and recombine in the CNT. Figure 1b illustrates the band bending in the carbon nanotube for a gate voltage between the voltages at source and drain. At $V_g = 1/2\ V_d$, we expect equal electron and hole currents to tunnel from opposite contacts through the thin Schottky barriers into the CNT.[6] The assumption of equal number of electrons and holes at $V_g = 1/2\ V_d$ is strictly valid for a symmetric device with mid-gap band lineup such as our laser-ablation grown nanotube devices. Longer devices such as the CVD tubes are more likely to be affected by hysteretic effects[10,11] that will lead to deviations from the above condition. To reduce the stress on the devices during the measurements, the drain voltage V_d is ramped between 0 V and $V_{d,max} \sim -10$ V on a time-scale of 5 s, while the gate voltage is set to a value around $V_g = 1/2\ V_{d,max}$. Typical transport currents under these conditions are between 1 and 5μA. Figure 1c shows the band structure for a (11,9) nanotube with characteristic 1-dimensional van-Hove singularities. Under the above biasing conditions, electrons are present in the conduction band *and* holes populate the valence band. The recombining electrons and holes produce the observed electroluminescence. Figure 1d shows an IR image of an actual device under external illumination. Probes (marked S and D) are touching large contact pads with

* Corresponding author. E-mail: avouris@us.ibm.com.
† IBM Research Division, T. J. Watson Research Center.
‡ Carbon Nanotechnologies, Inc.
§ Brookhaven National Laboratories.
|| Current address: Université de Montréal, C. P. 6128, succursale Centre-ville, Montréal (Québec) H3C-3J7.

10.1021/nl049607u CCC: $27.50
Published on Web 04/23/2004

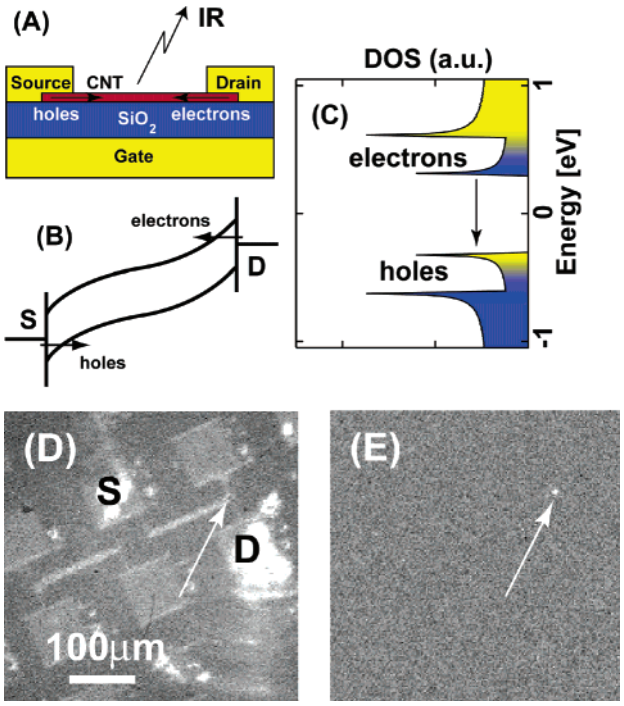

Figure 1. (A) Schematic of the device. The CNT is contacted with source and drain electrodes. Degenerately doped silicon separated from the tube by a 100 nm thick SiO_2 layer is used as a backgate. Electrons that are injected at the drain and holes that are injected at the source recombine radiatively in the carbon nanotube. (B) Schematic of the band bending in the CNT at $V_g = 1/2\ V_d$. The device behaves ambipolar with electron injection at the drain D and hole injection at the source S. (C) Density of states for a typical semiconducting nanotube. (D) IR image of the device with external illumination. Probes touching the source S and drain D pads and the connections leading to the CNTFET are visible. An arrow marks the position of the nanotube. (E) IR light emission around $\lambda = 1600$ nm from the same device biased with $V_d = -11$V and $V_g = -5.5$ V.

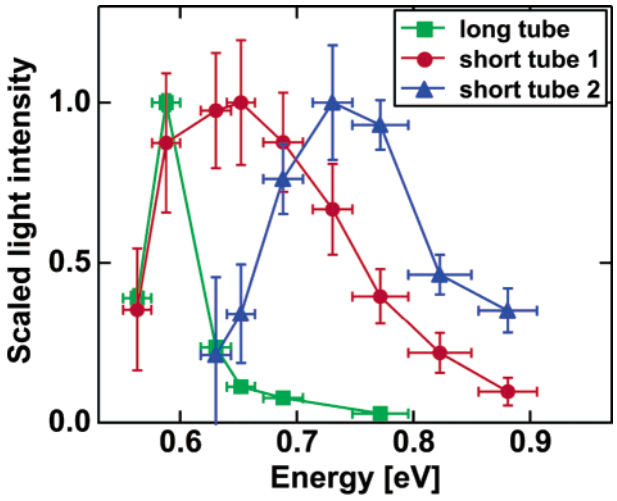

Figure 2. Emission spectra of three CNT-FETs: device ■ (green) is a 50 μm long tube; devices ● (red) and ▲ (blue) are ~ 500 nm short tubes. Biasing conditions: device ■ (CVD), drain = −20 V, gate = −10 V, $I = 3.5\ \mu$A; device ● (laser ablation), drain = 5 V, gate = 2.5 V, $I = 5\ \mu$A; device ▲ (laser ablation), drain = −11 V, gate = −5.5 V, $I = 900$ nA).

electrodes leading to the carbon nanotube (marked with an arrow). Figure 1e shows the same sample area in the dark with the device biased as described above. IR emission is observed at the position of the carbon nanotube.

Figure 2 shows the IR emission spectra of three different CNT-FETs. The low-energy emission onsets are at 0.58 eV (■ and ●) and 0.69 eV (▲). A comparison with fluorescence experiments suggests nanotube diameters of 1.8 and 1.5 nm.[12] Laser ablation grown nanotubes have a broad diameter distribution, centered around 1.4 nm. In our measurements, however, we are biased toward the larger-diameter tubes with small band-gaps, because we need to inject both electrons *and* holes at the same time and at a high rate to see electroluminescence. The inferred diameter for the CVD tube (■, 1.8 nm) is in good agreement with expected CVD tube diameters.

We now turn to the widths of the spectral peaks. Recent photoluminescence measurements on SWNTs dispersed in micelles showed peaks with fwhm ~ 25 meV.[13−15] In contrast, the electroluminescence line shapes are strongly device structure dependent. The green spectrum (■) was obtained from a 50 μm long CNT-FET, while the red and blue spectra (● and ▲) were measured on ~500 nm short devices. Long-channel devices show narrow peaks, while short-channel devices show broad and asymmetric peaks. We note that the emission from the long-channel device (■) is intrinsically even narrower, since the finite filter widths of our detection system (horizontal error bars) become comparable to the intrinsic width. The intrinsic width is close to what is observed in photoluminescence ~25 meV. Short-channel devices, on the other hand, have widths (fwhm) ~150 meV, after taking into account the spectral resolution of our measurement system. We confirmed that the widths of the emission peaks do not depend on the specific growth process (CVD or laser ablation) or sample preparation method (with or without LTO capping).

To evaluate the spectra, we consider the carrier thermalization processes in photo- and electroluminescence. High field transport measurements involving metallic nanotubes of varying lengths[16,17] suggest phonon scattering times of $\tau_{op} \approx 20$ fs for optical (or zone-boundary) phonons and $\tau_{ac} \approx 400$ fs for acoustical phonons. We compare these values to estimated carrier transit times of around $\tau_{short-chan} = 600$ fs in short CNTs, $\tau_{long-chan} = 60$ ps in long CNTs, and to reported photoluminescence lifetimes $\tau_{photolum} \approx 1-10$ ps.[18] Photoluminescence occurs from fully vibrationally relaxed states leading to narrow emission spectra. In long CNTs, electroluminescence should also involve relaxed carriers since the transit times are long compared to all the relaxation processes. In short CNTs, however, the transit time does not permit the thermalization of the injected carrier distribution below the energy of the optical/zone boundary phonons (~180 meV) because acoustic phonon scattering is too slow. The short-tube electroluminescence spectra are thus particularly interesting since they probe the distribution function of hot electrons on the femtosecond time scale.

To calculate the optical properties, we evaluate the imaginary part of the dielectric function for light polarized

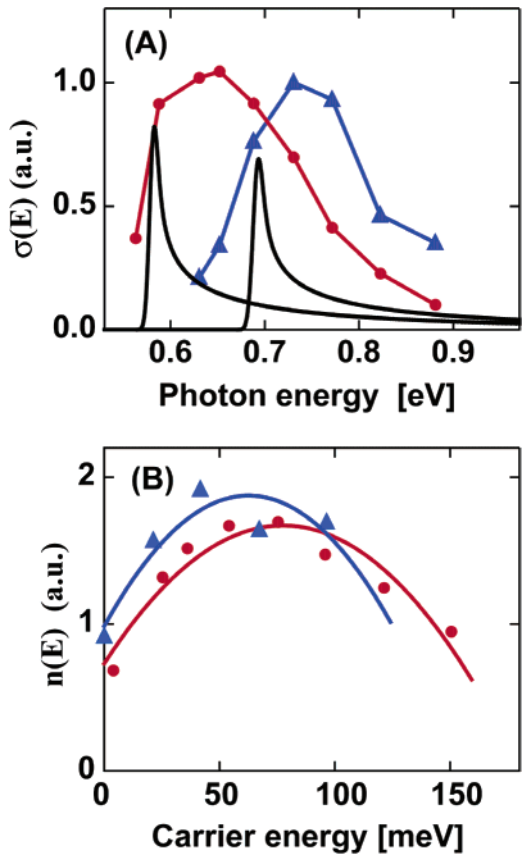

Figure 3. (A) Experimental spectra of the short-channel devices in Figure 2 and tight-binding calculations of the optical conductivity eq 1 for nanotubes with band gap 0.58 and 0.69 eV (−). (B) Hot carrier distribution in the two carbon nanotubes.

along the nanotube axis:

$$\epsilon_2(\omega) = \frac{8\pi^2 e^2}{Vm^2\omega^2}\sum_k P_{cv}{}^2(k)\delta(\hbar\omega - \Delta_k) \qquad (1)$$

where $P_{cv}(k)$ and Δ_k are the dipole matrix element and the band gap, calculated in the tight-binding model Hamiltonian approximation.[19] The dipole matrix element $P_{cv}(k)$ is proportional to the momentum (k) derivative of the tight-binding Hamiltonian in k-space,[20] such that it's magnitude is proportional to a hopping matrix element ($t = 3.0$ eV) and the C−C bond length ($a = 1.44$ Å). Figure 3a shows the experimental data of the short-channel devices alongside the calculated optical conductivity $\sigma(\mathrm{E}) = (\omega/4\pi)\epsilon_2$ (solid curve), which is dominated by the characteristic 1D Van-Hove singularities. We extract the carrier distributions $n(E)$ and $p(E)$ for electrons and holes in Figure 3b from the experimental data $f(E')$ and the calculated optical conductivity $\sigma(E')$ (Figure 3a) in the following way:

$$n(E)\cdot p(-E_{\mathrm{gap}} - E) = f(E_{\mathrm{gap}} + 2E)/\sigma(E_{\mathrm{gap}} + 2E) \qquad (2)$$

We assume equal occupancy of states for electrons and holes, i.e., $n(E) = p(-E_{\mathrm{gap}} - E)$, which is reasonable in the case of ambipolar CNT-FETs at $V_{\mathrm{gate}} = V_{\mathrm{drain}}/2$ where electron and hole currents are matched.[6] The distributions for the two devices are very similar with low occupancy at the band edges, a broad peak at 75 meV, and no measurable occupation of states above ∼180 meV. To our knowledge, this is the first measurement of the hot carrier distribution in a CNT-FET. The energies of the optical/zone boundary phonons in CNTs are around ∼180 meV, explaining the cutoff in the carrier distribution. A partial thermalization of carriers with energies <180 meV through acoustic phonon scattering is consistent with the broad maximum at 75 meV.

We now address the question of the efficiency of the radiative e−h recombination. For this purpose we measured the emitted light from the CNT-FET by integrating over the emission spectrum. We assumed equal electron and hole injected currents[6] and calibrated our detector and IR collection optics against emission from a known blackbody emitter. We thus obtained electroluminescence efficiencies around $\eta_{\mathrm{el-lum}} \sim 10^{-6}$ photons per injected e−h pair for laser ablation grown nanotubes and $\eta_{\mathrm{el-lum}} \sim 10^{-7}$ for CVD grown nanotubes. In nanotubes with small band gaps, such as most CVD tubes, nonradiative recombination through multiple phonon emission is faster, leading to a reduced efficiency of the radiative recombination process. We note that in long devices most injected carriers recombine (radiatively or nonradiatively) in the nanotube channel because recombination times are short compared to transit times. In short devices, however, this is not the case, and a fraction of the injected carriers can reach the opposite contacts without recombination.

Recent measurements of the efficiency in photoluminescence η_{photolum} for nanotubes in micelles yielded values between 10^{-3} and 10^{-5}.[13,15] The electroluminescence yield should be reduced because, in the absence of phonon participation, radiative recombination is possible only when the sum of the momenta of the electron and hole is zero. Phonon-assisted light emission processes allow electron−hole radiative recombination with a nonzero e−h momentum conserved by an emitted or absorbed phonon. This process should be especially important for hot-carrier recombination in short devices. We also note that only a quarter of the e−h collisions statistically would have the correct spin to give a radiative singlet state. Due to the presence of multiple carriers, Auger processes might further reduce the radiative efficiency. It is worth noting, however, that the photoluminescence from CNTs was found to be unobservable[21] for CNTs in direct contact with a silicon-oxide substrate (as in our case), so a significant enhancement of the electroluminescence yield might be possible by using suspended nanotube structures.

In conclusion, we have measured the spectrum and the efficiency of infrared emission from ambipolar carbon nanotube field-effect transistors. In long-channel devices the carriers thermalize before recombining and the spectra are narrow, whereas in short-channel devices we observe hot-carrier recombination with broad spectra. The extracted carrier distributions are explained in terms of phonon scattering, and we find that optical phonon scattering is effective in all devices, while acoustic phonon scattering,

that can fully relax the carriers, is only effective in long-channel devices. The efficiency of the radiative recombination is between 10^{-6} and 10^{-7} photons/electron−hole pair, but a substantial increase might be possible in suspended structures.

Acknowledgment. We are very thankful to Qiang Fu and Jie Liu from Duke University for providing CVD grown nanotubes and to Bruce Ek and Megumi Kinoshita for expert technical support. This research was performed partially under the auspices of the U.S. Department of Energy, Division of Materials Sciences, Office of Basic Energy Sciences under Contract No. DE-AC02-98CH10886.

References

(1) Avouris, Ph.; Appenzeller, J.; Martel, R.; Wind, S. J. *Proc. IEEE* **2003**, *91*, 1772−1784.
(2) McEuen, P. L.; Fuhrer, M. S.; Park, H. *IEEE Trans. Nanotechnol.* **2002**, *1*, 78−85.
(3) Misewich, J. A.; Martel, R.; Avouris, Ph.; Tsang, J. C.; Heinze, S.; Tersoff, J. *Science* **2003**, *300*, 783−786.
(4) Freitag, M.; Martin, Y.; Misewich, J. A.; Martel, R.; Avouris, Ph. *Nano Lett.* **2003**, *3*, 1067−1071.
(5) Martel, R.; Derycke, V.; Lavoie, C.; Appenzeller, J.; Chan, K. K.; Tersoff, J.; Avouris, Ph. *Phys. Rev. Lett.* **2001**, *87*, 256805.
(6) Radosavljevic, M.; Heinze, S.; Tersoff, J.; Avouris, Ph. *Appl. Phys. Lett*. **2003**, *83*, 2435−2437.
(7) Clifford, J. P.; John, D. L.; Pulfrey, D. L. *IEEE Trans. Nanotechnol.* **2003**, 2, 181−185.
(8) Derycke, V.; Martel, R.; Appenzeller, J.; Avouris, Ph. *Appl. Phys. Lett*. **2002**, *80*, 2773−2775.
(9) Javey, A.; Guo, J.; Wang, Q.; Lundstrom, M.; Dai, H. *Nature* **2003**, *424*, 654−657.
(10) Fuhrer, M. S.; Kim, B. M.; Duerkop, T.; Brintlinger, T. *Nano Lett.* **2002**, *2*, 755−759.
(11) Radosavljevic, M.; Freitag, M.; Thadani, K. V.; Johnson, A. T. *Nano Lett.* **2002**, *2*, 761−764.
(12) Weisman, R. B.; Bachilo, S. M. *Nano Lett.* **2003**, *3*, 1235−1238.
(13) Bachilo, S. M.; Strano, M. S.; Kittrell, C.; Hauge, R. H.; Smalley, R. E.; Weisman, R. B. *Science* **2002**, *298*, 2361−2366.
(14) Hagen, A.; Hertel, T. *Nano Lett.* **2003**, *3*, 383−388.
(15) Lebedkin, S.; Hennrich, F.; Skipa, T.; Kappes, M. M. *J. Phys. Chem. B* **2003**, *107*, 1949−1956.
(16) Javey, A.; Guo, J.; Paulsson, M.; Wang, Q.; Mann, D.; Lundstrom, M.; Dai, H. *Phys. Rev. Lett.* **2004**, *92*, 106804.
(17) Park, J. Y.; Rosenblatt, S.; Yaish, Y.; Sazonova, V.; Uestuenel, H.; Braig, S.; Arias, T. A.; Brouwer, P. W.; McEuen, P. L. *Nano Lett.* **2004**, *4*, 517−520.
(18) Ostojic, G. N.; Zaric, S.; Kono, J.; Strano, M. S.; Moore, V. C.; Hauge, R. H.; Smalley, R. E. *Phys. Rev. Lett.* **2004**, *92*, 117402.
(19) Saito, R.; Kataura, H. In *Carbon Nanotubes: Synthesis, Structure, Properties and Application*; Dresselhaus, M. S., Dresselhaus, G., Avouris, Ph., Eds.; Springer-Verlag: Heidelberg, 2001; Vol. 80.
(20) Johnson, L. G.; Dresselhaus, G. *Phys. Rev. B* **1973**, *7*, 2275−2284.
(21) Lefebvre, J.; Homma, Y.; Finnie, P. *Phys. Rev. Lett.* **2003**, *90*, 217401.

NL049607U